ADDITIVE MANUFACTURING AND STRESS ANALYSIS OF NATURALLY AND ARTIFICALLY OBTAINED CELLULAR STRUCTURES

by

SACHIN JOSE

Presented to the Faculty of the Graduate School of

The University of Texas at Arlington in Partial Fulfillment

of the Requirements

for the Degree of

MASTER OF SCIENCE IN MECHANICAL ENGINEERING

THE UNIVERSITY OF TEXAS AT ARLINGTON

December 2015

Acknowledgements

I would like to express my gratitude to my advisor Dr. Ashfaq Adnan, for his patience, support, and words of encouragement through the entire journey of my Masters program. I wish to thank him for guiding me in the research. He not only guided me but motivated me in every step, respected my ideas and treated me and every other student in the MMPL as a family.

I am very thankful to Kermit Beird for helping me with the tooling. I am grateful to all the staff at The University of Texas at Arlington, for their support and words of encouragement during my graduate study—Debi Barton, Lanie Gordon, Kathleen Priester, and Sally Thompson.

I wish to express special thanks to Md Farzad Sarkar for his help in obtaining cellular structure of bone, also to Sajith Anantharaman for his help in obtaining topology optimized structures and to all the other members of MMPL

I also wish to express my sincere gratitude to my parents who always believed in me and supported me during my Masters program

Above all, I am grateful for God for endowing me health, patience and knowledge to complete this book.

November 23, 2015

Abstract

ADDITIVE MANUFACTURING AND STRESS ANALYSIS OF TOPLOGY OPTIMIZED CELLULAR STRUCTURES

Sachin Jose, MS

The University of Texas at Arlington, 2015

Supervising Professor: Adnan Ashfaq

The main objective of our research is to manufacture topology optimized cellular structures using 3D printing and polymer infusion and obtain their structural response. First, we have obtained topology optimized cellular structure of beam using an in-house topology optimization tool. The Solid Isotropic material with Penalization (SIMP) method of optimization is used for finding the optimal topology. Since we require a continuous structure where we can take advantage of additive manufacturing, a no-penalty approach was chosen. For 3D printing, first the optimized condition for manufacturing was determined. Important parameters on which manufacturing depend are Number of Shells, Infill percentage and Layer thickness. Then we manufacture the optimized structures using Fused Deposition Modeling. Next we fill the voids of the structures using polyurethane foam. The performance of the structures are first assessed by performing static tensile/compression test followed by bending tests and also by using Finite element based stress analysis in ABAQUS

Table of Contents

List of Illustrations

List of Tables

Chapter 1

Cellular Structures

Cellular structures have been drawing increasing attentions in recent years due to their potentials in high performance-to-weight ratio applications. Sometimes referred to as “metamaterials”, cellular structures could achieve tailored physical and mechanical properties via the control of interior geometries [14-16]. Additive manufacturing (AM) has been increasingly often used to manufacture cellular structures due to its freeform capability with complex geometries [17-20].On the other hand, the design theory for cellular structures is relatively underdeveloped, especially for the cellular structures with 3D architectures. It has been suggested that the development of design tools for 3D cellular structures could be facilitated by AM technologies [21]. The fabrication capability of AM enables verification of cellular design by experimentation, identification and investigation of other non-geometrical design considerations like manufacturing and boundary factors.

The concept of designed cellular materials is motivated by the desire to put material only where it is needed for a specific application. From a mechanical engineering viewpoint, a key advantage offered by cellular materials is high strength accompanied by a relatively low mass. [11] [12].

As the materials are only added in places where they are absolutely essential, it helps to build light weight structures. Few of its applications are as follows:

1. Aircraft Industry- These structures can be used in places where secondary structures are required like the handles of cabin bag section, arm rest and so on.
2. Naval Application. Example see Figure 1-1

Figure 1-1 Cellular Structure in naval application [22]

1.1 Approach

There are various cellular structures that exist in nature. Our research focuses on obtaining natural and artificial cellular structures and to find ways to improve their mechanical properties. For naturally obtained cellular structure, a CT scan image of bone was used and by using a set of predefined process a STL file was generated. This work was done by a PhD student; Md. Farzad Sarkar from University of Texas at Arlington. Artificial Cellular Structures were made using topology optimization. This was done with the help of finite element analysis and MATLAB. SIMP approach was used for optimization. This work is properly illustrated by Sajith Anatharaman [10]

Once the design was obtained, the next big step was to manufacture these structures. 3D printing has come a long way since it was first introduced in the early 1980s. If there is any design that a designer can make then there is a 3D printer that can manufacture it. Additive manufacturing was done with the help of a 3D printer. First step was to optimize the manufacturing condition in a 3D printer. This was done using Design of Experiments where sample structures were manufactured by varying different parameters which is explained in Chapter 2.2. Next step was to manufacture both artificial and natural cellular structure using this optimized condition. Next step was to

perform mechanical test on these structures. But there is a possibility that the cellular structures might break due to buckling when a compressive load is applied and hence it will be tough to gauge its actual properties. Hence we used polyurethane foam to fill the void space. Mechanical tests were carried on both structures with and without polyurethane foam to get a direct comparison. Further Finite Element Analysis was carried out on these structures using ABAQUS.

Chapter 2

Additive Manufacturing

Additive Manufacturing is also known as layer manufacturing. In additive manufacturing structure is build layer by layer whereas subtractive manufacturing is used in most of the conventional methods i.e. manufacturing by removal of material. Development in the field of additive manufacturing focuses on building complex parts which can be used in aerospace, automotive, naval and medical applications [10]. One of the main advantage additive manufacturing has over the methods is that the designer does not have any constraints while designing the domain. Earlier the designer had to factor in the feasibility of manufacturing process while designing a structure. However due to additive manufacturing designer can design any complex part as it can be manufactured with ease.

We used a MakerBot replicator 2X 3D printer for additive manufacturing.. It is the most basic form of 3D printing. This chapter will provide the readers with a brief idea about history of 3D printers and the design of experiments carried out to find the optimized manufacturing conditions.

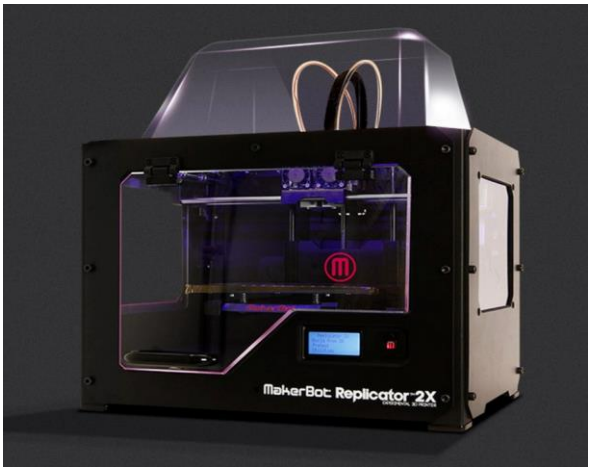

Figure 2-1 MakerBot Replicator 2X 3D printer

2.1 History of 3D Printers

3D printer was first introduced in the early 1980s. It was called as rapid prototyping. This was because these processes were used to generate prototypes for product development within industry [23]. First Patent for Sterelithography Apparatus (SLA) was filled in 1986 by Charles Hull. Later on in 1987 Carl Deckard filled a patent for Selective Laser Sintering (SLS) process. Fused Deposition Modeling which is used in MakerBot replicator 2X was founded by Stratasys Inc. In late 1990's and early 2000's a variety of new technologies were introduced which focused on industrial applications, R&D was also being conducted by advanced technology providers for tooling direct manufacturing applications.

FDM is a layer by layer process in which a heated filament is fused out through the nozzle depositing material. Two plastic elements used in 3D printer are Acrylonitrile Butadiene Styrene (ABS) and Polylactic Acid (PLA), which are available in the sizes of 1.75mm and 3mm. We use plastic filament of 1.75mm for testing. The plastic filament is fed to the nozzle of the extruder where it gets heated up. The nozzle follows a predefined tool path and deposits material on the heated bed i.e. the build plate

2.2 Optimized Manufacturing Condition

In order to manufacture the best quality product it is important to find out the optimized condition at which the machine will give the best output. Few of the parameters which affects the MakerBot replicator 2X are rastor angle, layer thickness, raster to raster air gap, number of shells and infill percentage. Out of these the key parameters were Layer thickness, infill percentage and number of shells

A set of experiments were carried out in order to find the optimized condition. Seven (7) sample structures were manufactured such that in two of them the number of shells was varied and the rest were kept at default optimum value, in the next 3 infill

percentage was varied between 15% to 100% and in the last two layer thickness was varied. Default optimum values were number of shells as 2, infill percentage as 10 and layer thickness as 0,15mm.

Tensile test was carried out on all these structures using universal testing machine at Micro Mechanics and Physics Lab. Force was applied at the speed of 1mm/min and it was stopped when the specimens was split into two. Trapezium X software records all the data as the test was carried out and these data was used to plot the stress strain graph.

(a) (b)

Figure 2-2 a) Sample structure b) Tensile test

2.2.1 Effect of number of shells

Number of shell means the amount of time the machine goes around the perimeter of object depositing 100% infill each time. It was varied between 2 and 25. The base condition for a high resolution object is infill should be 100%, layer thickness should be 0.1mm. The figure 2-3 shows how stress varies when number of shell is increased.

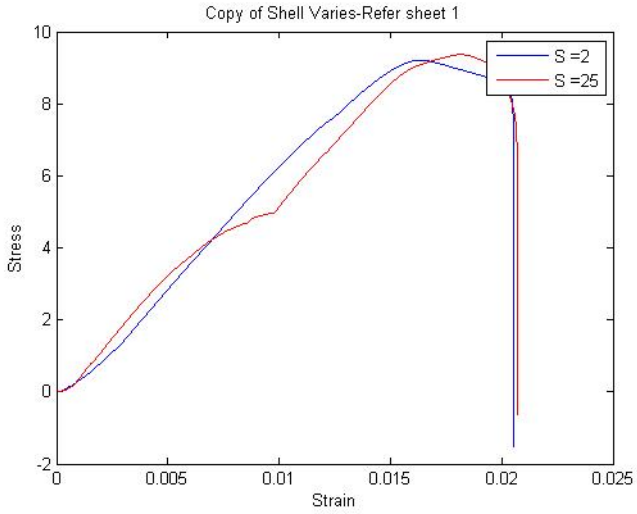

Figure 2-3 Stress-Strain graph for effect of number of shells

Shell 25 has higher stress mainly because of the fracture it developed at the centre. Basically when number of shell is increased it means that the infill is 100% for that many number of times the machine goes round the perimeter. The same result can be obtained by keeping infill 100% and number of shells as 2, thus we can avoid the fracture at the centre.

2.2.2 Effect of Infill percentage

Infill refers to the deposition inside the material. 100% infill means that there are no void spaces inside and as infill percentage is reduced, void spaces are created. Infill amount was varied between 15% to 100%. Rest of the parameters were kept same as the high resolution condition i.e. number of shell as 2 and layer thickness as 0.1mm.

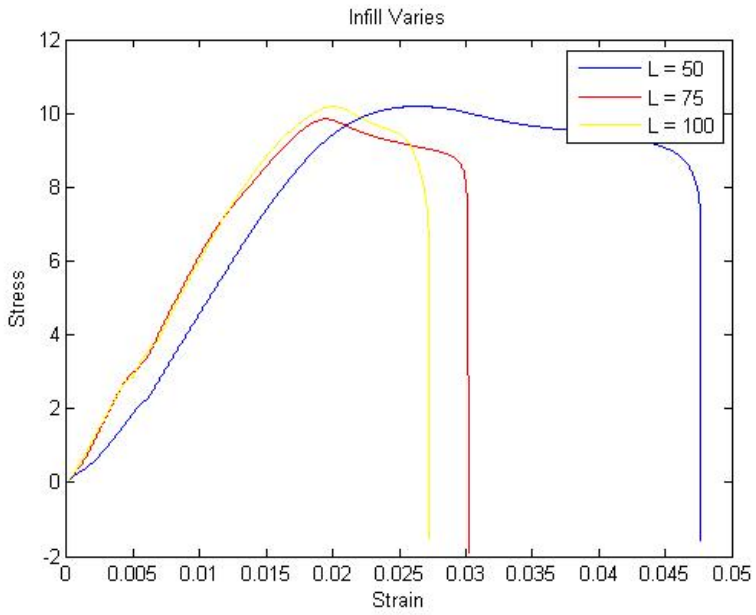

Figure 2-4 Stress-Strain for effect of Infill percentage

The result shows that as infill is varied stress increases. It is highest for 100% infill, which means that infill should be kept at maximum for us to obtain best results.

2.2.3 Effect of Layer Thickness

Suppose we are developing a structure of 20mm and layer thickness is kept as 2mm, then it means that in each pass it will build the structure up by 2mm. Increasing layer thickness implies reducing the number of passes. Therefore, layer thickness was varied in order to find out the stress variation.

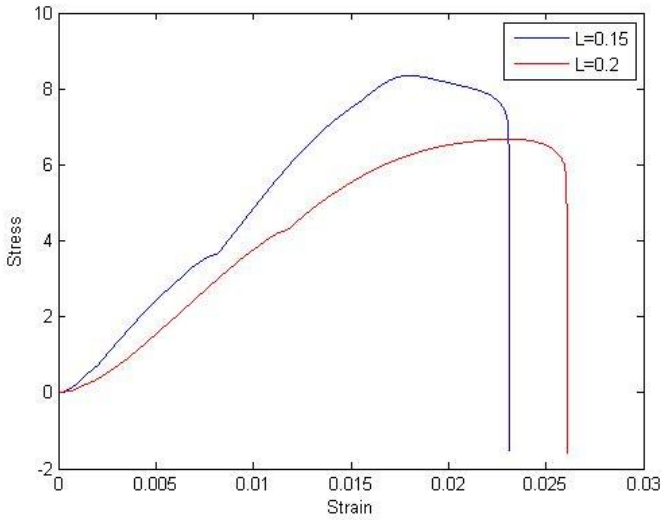

Figure 2-5 Stress-Strain graph for effect of layer thickness

Graph 2.5 shows that stress is highest when layer thickness is kept at least at possible. Hence a layer thickness of 0.10mm should be preferred.

2.2.4 Conclusion

Table 2-1 Maximum Tensile Force

		Maximum Force (N)
Shell Varies	S-2	274
	S-25	280
Infill varies	I-50	308
	I-75	298
	I-100	310
Layer Varies	L-0.15	249
	L-0.2	192

Table 2-1 shows that the maximum force of 300N is applied to the structure which has the following parameters: number of shells - 2, infill - 100% and layer thickness – 0.15mm. Hence this optimized condition will be used to manufacture all the structures henceforth in this book

Chapter 3

Polyurethane Foam

Consider a thin long rod of aluminum subjected to a compressive load. Aluminum has a very high compressive strength. However, since the rod is long it could fail in between due to buckling. So even though we obtain a low value of compressive strength experimentally, it is not the true compressive strength. By providing support to the region which undergoes buckling, this issue can be resolved and true compressive strength of aluminum can be obtained. Similar logic can be applied to the naturally and artificially obtained cellular structures. These structures when subjected to compressive load may break at a low value due to buckling. Hence these structures cannot be used for their intended purposes. There is a need use a different material to fill up the void spaces and support these structures so that one can obtain its true compressive strength. Important properties while choosing these materials are:

1. Light weight
2. Low Density
3. High compressive strength

Polyurethane Foam is known for its low density and good mechanical strength. They can be used as insulating materials. They can also be used as core materials of sandwich constructions [1]. There are various articles which shows the effect of foam density on mechanical properties of Polyurethane Foam [2,5]. Different production technologies decide on intrinsic structure and foam density and this determines the capacity to carry mechanical loads. Hence it is dependent on different foam producers. For this reason, we will be carrying out some mechanical testing on the polyurethane foam to analyze its mechanical properties.

3.1 Manufacturing of Polyurethane Foam

Polyurethane Foam was obtained from US Composites. It consists of two parts: part A and B. When it is mixed in the right proportion it expands to 15 times its volume. Figure 3-1 shows a step by step guide for the manufacturing of polyurethane foam.

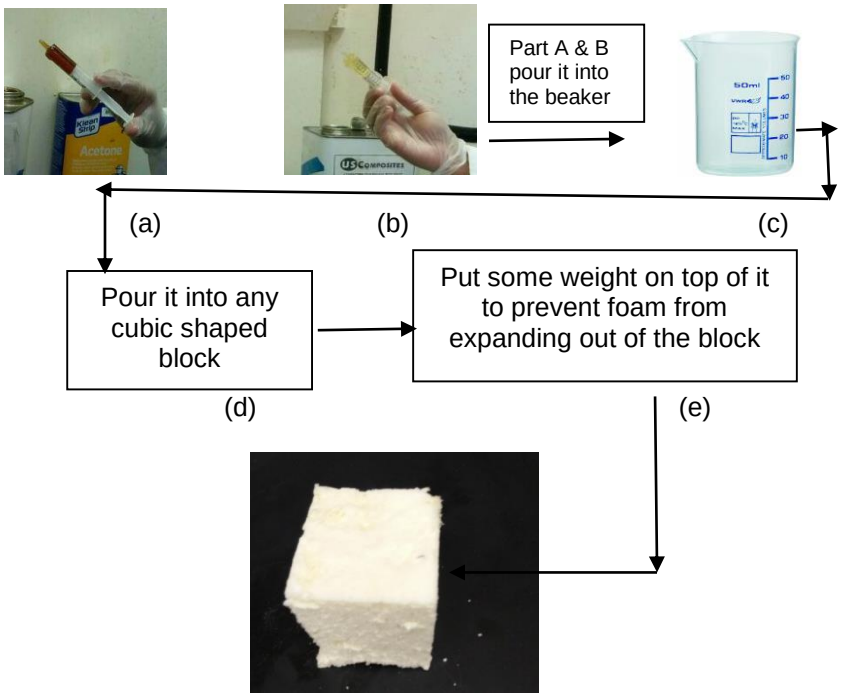

Figure 3-1 Steps to manufacture polyurethane foam a) Polyurethane Foam part A b) Polyurethane foam part B c) Beaker d) Pour the mixture into the structure e) Clamp the structure f) example of a polyurethane foam

Steps to manufacture polyurethane foam:

1. Find out the required volume to be filled up by polyurethane foam eg 150 cc^3
2. Divide it by 15. Therefore required volume of polyurethane foam is 15 cc. (convert it into ml)

3. Take equal parts of Polyurethane part A and B and mix it in a beaker for 20 sec as shown in Fig 3-1 (a-c).
4. Pour this mixture into the structure/ cubic block within 25 sec.
5. Clamp the structure down or place some weight on top of it to prevent the polyurethane foam from expanding out of the block.
6. Figure 3-1 (f) shows a sample of light weight polyurethane foam.

3.2 Analyzing mechanical properties of polyurethane foam

Four samples were manufactured using the procedure mentioned in 3.1. Two samples were used for compression test to determine young's modulus and two of them were used to determine the Poisson's ratio.

3.2.1 Density of Polyurethane foam

One of the properties of polyurethane foam is that it has low density. Four samples which were manufactured for testing was weighed initially to find out the density. This data was important to cross check density of structure filled with foam and also to assert our claim that polyurethane foam has low density

$$Density = \frac{Weight}{Volume}.$$

Weight of the foam was measured using a weighing scale available at MMPL lab.

First sample had a weight of 3.1 gram and dimension of 3.5 x 2 x 3.26 cm.

$$Therefore\ Density = \frac{3.1}{3.5 * 2 * 3.26} = 0.135 \frac{g}{cc^3}$$

Similarly, for second, third and fourth structure, density was 0.148g/cc^3. 0.128g/cc^3 and 0.154g/cc^3

Density of 0.141g/cc^3 was the average of four readings can be used for all calculations.

3.2.2 Young's Modulus for Polyurethane Foam

In order to find the young's modulus, compression test was carried out on two of the samples using the Universal Testing Machine at Micro Mechanics and Physics Lab. It has trapezium X software which records all data. It records data for each sec and with the help of these data we can plot the force vs displacement graph and also the stress strain graph which will be used to find the young's modulus.

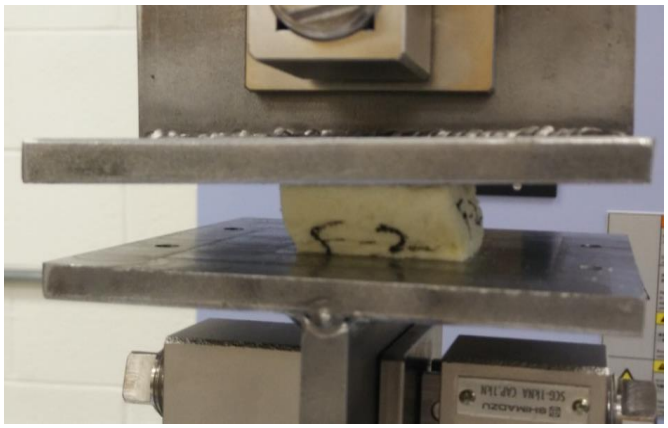

Figure 3-2 Compression of Polyurethane Foam

Polyurethane foam was compressed almost to half its length and yet it did not fail which shows that it can sustain a very high compressive load. Figure 3-3 shows the stress-strain graph which was used to evaluate the young's modulus. Young's modulus is determined along the linear portion of the graph where the deformation is not permanent.

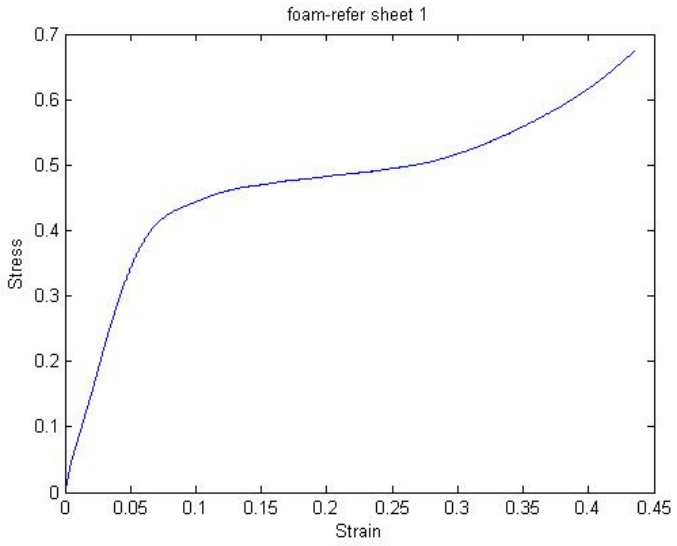

Figure 3-3 Stress Strain graph for Polyurethane Foam

$$Young's\ Modulus, E = \frac{Stress}{Strain}$$

A straight line is drawn alone the slope of the curve and slope of that straight line gives us the young's modulus. Value of young's modulus was found out to be 10N/mm^2 A close look at the stress strain graph shows that the material undergoes plastic deformation and this can be proved by Fig 3-4 (b) which shows the polyurethane foam in its deformed shape after compression.

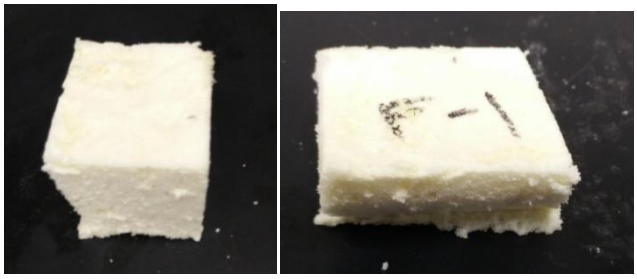

(a) (b)

Figure 3-4 (a) Before Compression (b) After Compression

3.2.3 Poisson's Ration

$$Poisson's\ Ratio\ (\nu) = \frac{Lateral\ Strain}{Longitudinal\ Strain}$$

In order to find out the Poisson's ratio, Lateral and longitudinal strain needs to be obtained first. Two samples were compressed using Universal Testing Machine. Lateral strain was found with the help of scale. One of the lengths was held using scale (as shown in figure 3-5) and the length was recorded. Now once the compression starts, the material will expand and the grip will move sideways in order to accommodate this deformation. New reading can be obtained from the scale. Figure 3-5 shows the method used to obtain lateral strain.

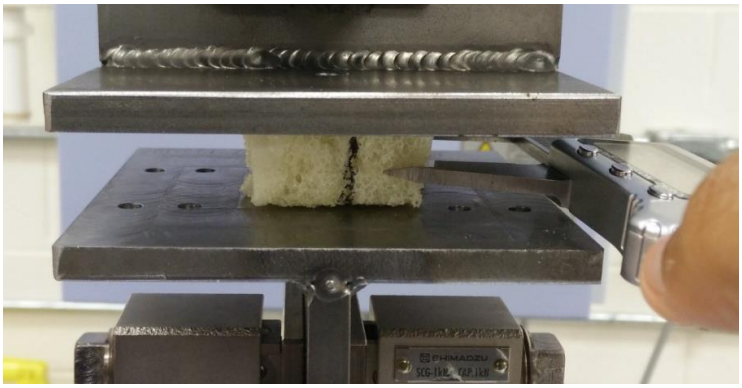

Figure 3-5 Evaluating Lateral Strain

$$Lateral\ Strain\ = \frac{Change\ in\ Length}{Original\ Length} = \frac{0.45}{30.6} = 0.0149$$

Longitudinal Strain was found out using the Trapezium X software which records the displacement as it gets compressed.

$$Longitudinal\ Strain\ = \frac{8.1676}{33.33} = 0.2449$$

$$Poisson's\ ratio = \frac{Lateral\ Strain}{Longitudinal\ Strain} = \frac{0.0149}{0.2449} = 0.06$$

Similar procedure was followed for the second sample. Poisson ratio was found to be 0.7

Chapter 4

Comparing Stiffness of Bone Like Structure

After Life evolved on earth, nature discovered low density cellular material. Bones use these light weight cellular materials to withstand the weight of the human body. One of the most important things that make vertebrates different from other animals is the bone. It has evolved over several hundred million years. Bone is something which can have the same strength as that of cast iron but at the same time it is as light as wood. This can be seen from the fact that the front leg of a horse can withstand the load generated by horse when it is running at a high speed. The upper arm is able to keep birds aloft when if flies. Deer uses their antlers as a weapon when it fights with other deer. It undergoes tremendous impact while fighting but yet it doesn't fracture [6].

Bone looks like a solid structure but in reality they are intricate sandwich structures which are made up of two parts. Dense outer shell is called cortical bone which forms the shaft of a long bone whereas the spongy part is called as trabecular. Figure 4-1 shows the cellular structure of a trabecular bone of a young normal person. It comprises of interconnected network of rods and plates. Rods are responsible for low density cells while plates produce virtually closed cells with higher density. Low density cells are open and are like rods. They become closed and like plates when density increases/Relative density of trabecular bone varies from 0.05 to 0.7

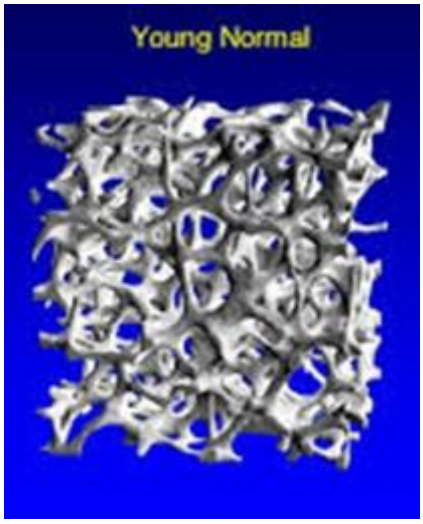

Figure 4-1 Trabecular structure of bone [7]

This study is performed to develop a structure that microstructure similar to that of bone and also to perform compression analyses in all the three directions to calculate their stiffness.

4.1 Manufacturing

The design of the bone structure was obtained from CT scan images of a 61 year old human femoral neck. CT scan is a non-destructive way to obtain the cross sections of an object. Micro CT scan indicates the cross sections in micro scale.In biomedical imaging converting micro CT scan images into three dimensional models is frequently used. The trabecular part was separated from the CT scan and converted into a three dimensional solid volume mesh using a set of predefined processes. A software program called NRecon was used to correct the long axis shift and grayscale.MIMICS, software used for Medical image processing was used to create a surface combining the corrected two dimensional images. Effective region of interest was selected from the grey scale area and converted to 3D surfaces. The obtained surfaces are modified to generate an inverted print of the structure that define mold suitable to molding the object. The surface

files were converted into STL format which contained the information related to surface of geometry [8].

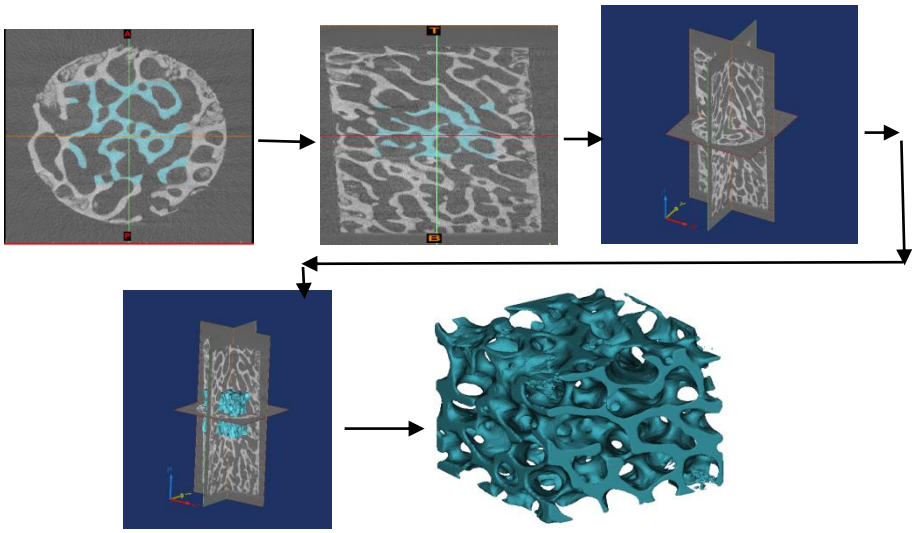

Figure 4-2 Obtaining Trabecular Structure of Bone from CT scan images [8]

MakerBot replicator 2X has makerbot software which will convert the STL file in to a.x3g format by which it can manufacture the structure. There are various parameters such as speed, temperature of extruder, temperature of bed plate which the user can vary depending on the material used. After importing the STL file, user will have to place the structure on the build platform. User can rotate the structure or scale it and manufacture it at any place on the build plate. Right or left extruder should be selected based on where the filament is loaded. ABS was used to manufacture the bone like structure hence the inbuilt MakerBot ABS filament was selected as the type of filament. By selecting ABS filament, temperature of extruder is automatically set to 230^{o}C, travel speed of extrusion is also set automatically. These parameters can be adjusted manually too. Once the settings are confirmed, it is saved, exported into a .x3g format and uploaded into a SD card which will be connected to 3D printer.

The print settings are as follows:

Resolution	:	High
Layer Thickness	:	0.15mm
Infill Percentage	:	100%
Number of Shells	:	2
Filament	:	MakerBot ABS filament
Temperature of extruder	:	230^{o}C
Build plate temperature	:	110^{o}C
Speed while travelling	:	150mm/s
Speed while extruding	:	90mm/s

ABS filament with a diameter of 1.75mm is set in the extruder. Once the extruder heats up, the nozzle deposits ABS to make a layer and the process was repeated in layer by layer fashion until the complete structure is built.

4.2 Testing

Using the microstructure obtained from Section 3.1, bone like structure was manufactured using MakerBot Replicator 2X. Figure 4-3 depicts the bone like structure. In order to find out the stiffness in each direction and also to analyze the effect of polyurethane foam, 6 structures were manufactured in all. Careful observation shows that the structure which has long horizontal line depicts Z- direction, structure which has a solid rectangular type outer surface depicts Y-axis and the structure which has curved like shape depicts X- direction. Out of the 6 structure, 2 of them were In X-direction, two in Y-direction and last two in Z-direction. Out of the two, one of them was filled with foam in each direction. Foam was filled using the procedure described in chapter 3. Table 4-1 shows the weight of the structure filled with and without polyurethane foam.

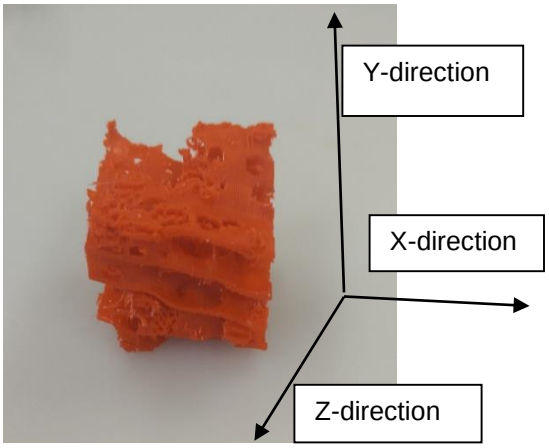

Figure 4-3 Bone Like Structure

Table 4-1 Weight of bone like structures

	Weight (g)	
	Without Foam	With Foam
X-direction	2.7	4.2
Y-direction	3.1	5.1
Z-direction	3.4	5.1

Compression test was performed on these structures using Universal Testing Machine at MMPL. It is a force controlled equipment and can compress the structure upto 5000N. Trapezium X software records the displacement as force increases and gives the output in excel form which can be later used to plot force-displacement graph. Figure 4-4 shows bone structure in X, Y and Z direction and also a bone like structure filled with polyurethane foam.

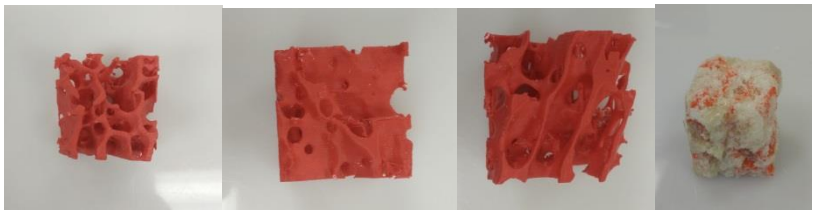

(a) (b) (c) (d)

Figure 4-4 Bone like structure in a)X-direction b)Y-direction c)Z-direction d)Filled with Polyurethane Foam

4.3 Results and Discussions

Figure 4-5 shows the Specific Strength for all the six structures. The Raw data extracted from the Trapezium X software gives the maximum force for each structure. Specific Strength is calculated using the following formula:

$$Specific\ Strength = \frac{Stress}{Density}$$

Following observations can be made from the graph.

1. Compressive strength of the structure is more in one direction as compared with others and this is because bones carry most of the loads in one direction and hence they develop higher load in that direction
2. Filling the void spaces with polyurethane foam has increased the compressive strength in all the three directions. This implies that the cellular structure was initially breaking at a lower load because of buckling. Polyurethane foam is able to support the structure and it gives a true indication of compressive strength.

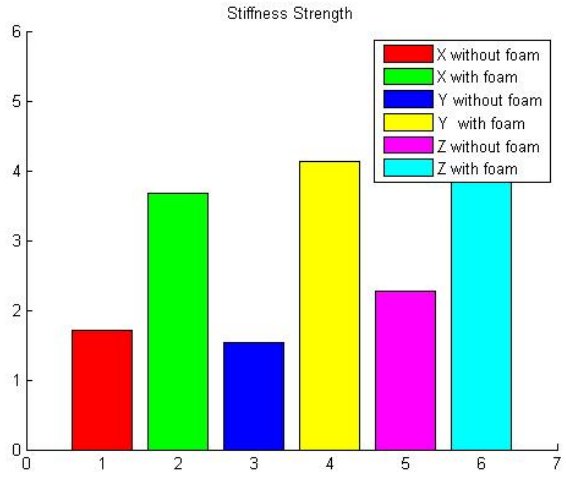

Figure 4-5 Specific Strength of 6 bone like structures

Figure 4-6 compares the young's modulus, calculated from the linear portion of the stress strain graph for all the 6 structures. It is highest in the Z-direction with polyurethane foam. It is highest in the same structure which was able to sustain the maximum compressive force.

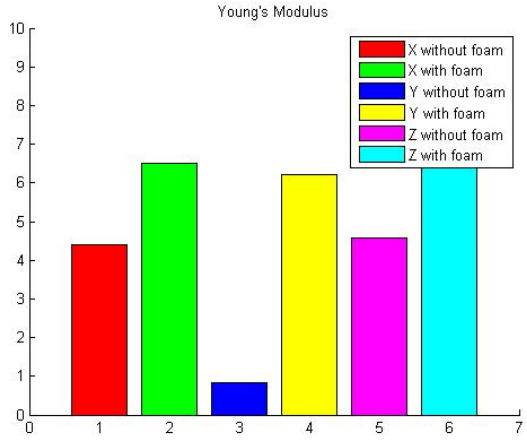

Figure 4-6 Young's Modulus for bone like structure

Chapter 5

Compression and Bending Analysis of Topology Optimized Structures

Topology optimization is a type of structural optimization where the problem is defined in a design domain. Boundary conditions and the optimization is done to achieve the necessary output satisfying all the constraints. There are different ways by which optimization can be obtained. SIMP was the method used in optimizing our structure. SIMP stands for Solid Isotropic Material with Penalization. It is based on power law method. Here the finite element formulation is kept fixed and each element in the design domain is associated with a function called density whose values vary between 0 and 1. The objective of the program is to find out this density function which would resemble optimal material distribution. The density of 0 and 1 can be viewed as void and solid material and those values between0 and 1 as grey regions. Figure 5-1 enlists the topology optimization procedure [10].

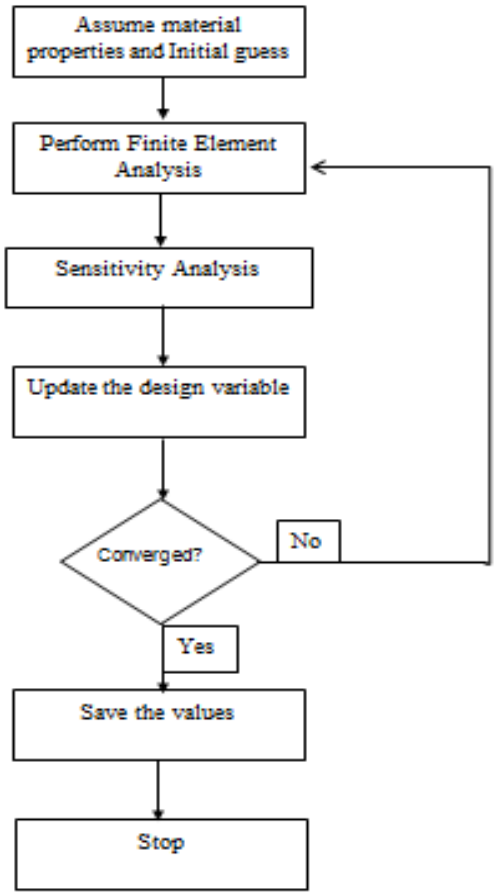

Figure 5-1 Topology Optimization Procedure [10]

Finite Element method was used for structural calculation. This was done in MATLAB. It uses the basic equation of Finite Element,

$$[F] = [K][U]$$

Where F is the force applied, K is the stiffness Matrix and U is displacement. Here all the parameters are considered as function of Density. For the topology optimized structure, a compressive load was applied on a rectangular block which was fixed at the bottom. Material was removed in the region where density was greater than 1. MATLAB gives a

output in the STL format. For conversion into STL format, densities were converted into hole dimensions. In this way, a topology optimized structure was designed [10]

5.1 Manufacturing of Topology Optimized Structures with polyurethane foam

To analyze the effect of polyurethane foam in topology structures, void spaces in few of the structures were filled with polyurethane foam. Steps followed were same as the procedure described in section 3.1 only difference being that topology structures were used in the place of cubic shaped holes. Initially volume required to be filled by polyurethane foam was calculated. It was then divided by 15 as foam expands up to 15 times and equal measures of part A and B were taken. For e.g. if 20 ml is required to fill up the entire structure then 10 ml of part A and 10 ml of part B were taken. Figure 5-2 shows the steps for infusion of polyurethane foam into the structure. It is ensured that the structure is clamped or placed on a flat plate initially and after infusion of foam it should be clamped from the other side too or some heavy weight needs to be kept on it so as to ensure that foam expands inside the void spaces.

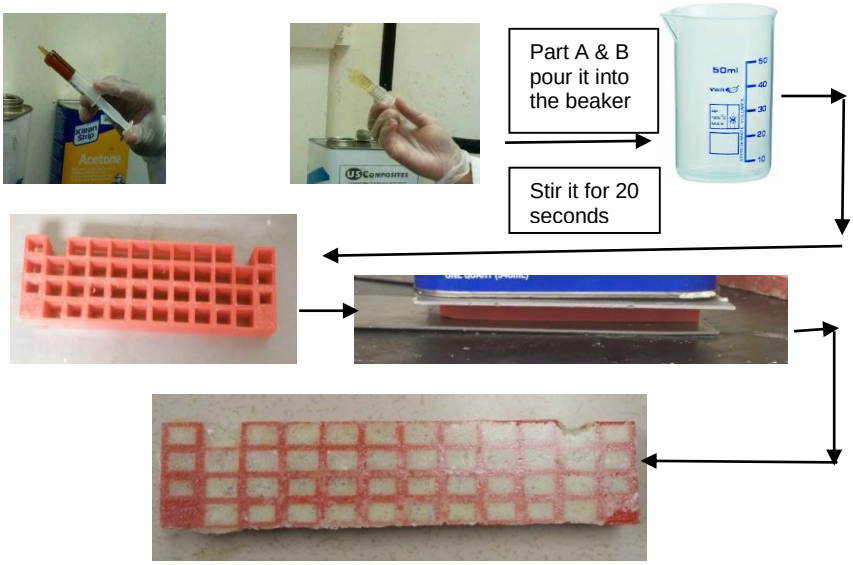

Figure 5-2 Infusion of Polyurethane foam into an optimized structure

5.2 Compression Test

Using the optimization code, topology optimized structure was manufactured using MakerBot Replicator 2X. In order to find out the compressive strength in each direction and also to analyze the effect of polyurethane foam, 6 structures were manufactured in all. Structures were varied in X, Y and Z direction by varying the direction of void spaces. In X-direction void spaces were more in number and it goes across the height of the structure i.e. for 0.5". In y- direction it goes across the breadth i.e for 1 inch and Z-direction has the least number of void spaces at it goes along the length of the structure i.e. for 4". Out of the 6 structure, 2 of them were In X-direction, two in Y-direction and last two in Z-direction. Out of the two, one of them was filled with foam in each direction. Foam was filled using the procedure described in chapter 3. Figure 5-3 shows the structure in X, Y and Z direction with and without polyurethane foam. Table 5-1 shows the weight of the structure filled with and without polyurethane foam.

Table 5-1 Weight of optimized structures for compression

	Weight (g)	
	Without Foam	With Foam
X-direction	12.8	16.3
Y-direction	13.3	16.2
Z-direction	12.9	15.7

(a) (b) (c)

(d) (e) (f)

Figure 5-3 Optimized structures in a)X-direction b)Y-direction c)Z-direction d) X-direction with foam e)Y-direction with foam f)Z-direction with foam

Compression Test was carried out on these structures using the universal testing machine at MMPL. It was tested till a first peak was observed. Speed was kept at 2mm/min.

Figure 5-4 Compression of an optimized structure in Y-direction

5.3 Results and Discussion

The graph in figure 5-5 shows the compressive strength of the structures. It shows that the structure in the Z-direction filled with polyurethane foam can withstand the maximum compressive force. It did not break even when a compressive force of 5000N was applied to it. Polyurethane foam was used in the structures to increase their mechanical strength. The graph shows that it has helped to increase the compressive strength. This means that the cellular structures which were breaking initially because of buckling are now able to sustain higher load because of polyurethane foam.

So the conclusion is that the structures should be filled with polyurethane foam for better mechanical properties and they can be used in industries where there is a need for light weight strong mechanical structures.

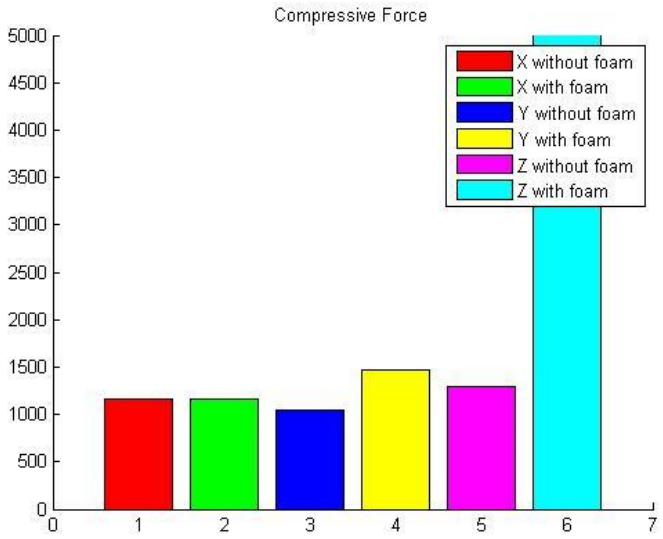

Figure 5-5 Compressive strength of optimized structures

5.4 Bending Test

6 structures were manufactured in order to find the effect of bending force in each direction and also to analyze the effect of polyurethane foam on each structure.

Same as for compression test, 2 structures were made in each direction. One of them was filled with foam. Table 5-2 shows the weight of the structures

Table 5-2 Weight of Structures for Bending test

	Weight (g)	
	Without Foam	With Foam
X-direction	13.1	16.8
Y-direction	13.3	16
Z-direction	13	15.5

Bending test was carried out using universal testing machine at MMPL. No standard fixture was available and hence a fixture was made for 3-point bending. Two rollers were attached on the bottom compression plate. There were 12.7mm in diameter and kept 55mm apart. Third roller was attached to the top compression plate and then they were aligned in such a way that the third fixture was in the center of the two bottom rollers. A maximum of 5000N force was applied. Testing was carried out till the structure breaks, It was carried out at a speed of 2mm/min. Figure 5-6 shows the bending test of optimized structures

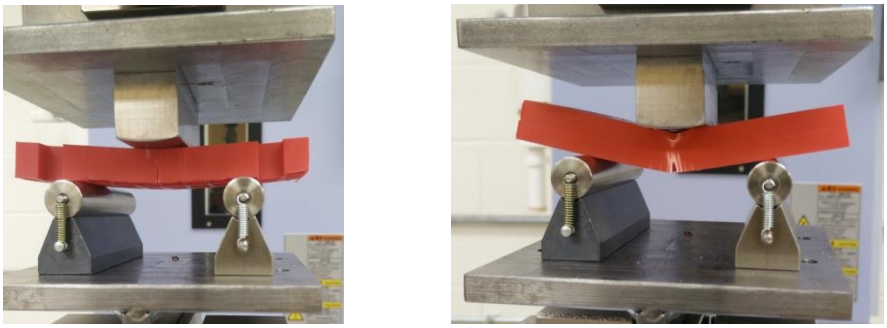

(a) (b)

Figure 5-6 Bending test of a) Optimized structure in X-direction b) Optimized structure filled with polyurethane foam in Z direction

5.5 Results and Discussion

Figure 5-7 shows values of bending force for topology structures with and without foam. The result shows higher bending force for the topology structure having void space. This implies that properties of the structure has improved because of polyurethane foam,

Void Spaces in Z-direction filled with polyurethane foam has the highest bending force. This is because of a larger moment of Inertia which acts on this structure. Structures with larger moment of inertia will be harder to rotate or bend. Result shows that with the help of polyurethane foam structures are able to sustain more bending force.

These structures are light in weight and at the same time have greater resistance to bending stress and ensure structural integrity. These can be used in places where high stiffness and low weight structures are required. They can be used in aircrafts where there is a need for lighter weight structures for fuel consumption and emission control.

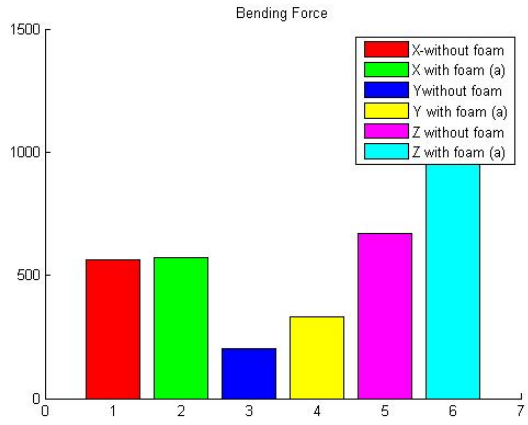

Figure 5-7 Bending force for optimized structure

Chapter 6

Finite Element Analysis using ABAQUS

Finite Element Analysis was carried out to find out how the structure cracks at a certain displacement and also to give an insight about how polyurethane foam is able to cushion the load and break at higher force and displacement.

6.1 Steps in FEA

1. Initially the STL output from Matlab is saved in the IGS format using Solidworks/PTCCreo. This file is then imported into Abaqus

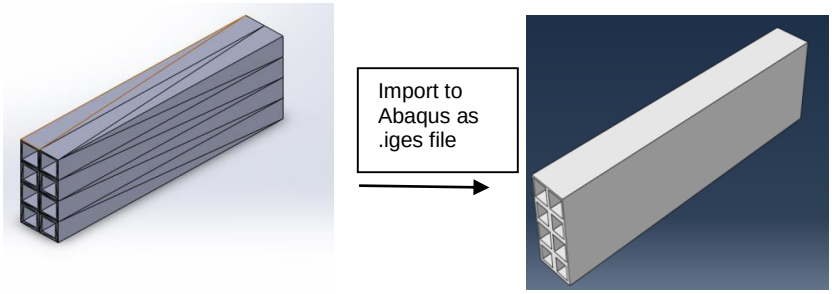

Figure 6-1 Importing Geometry

2. Imported Geometry has to be given certain parameters like 3D, deformable etc.

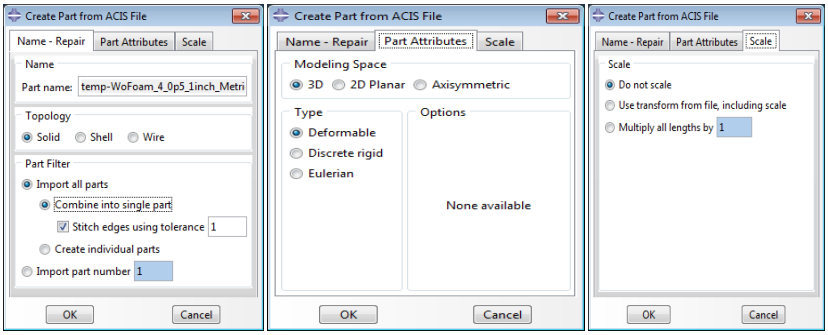

Figure 6-2 Parameters while importing Geometry

3. Next step is to input material properties and section assignment. Section assignment is done to assign material properties to that section (Structure)

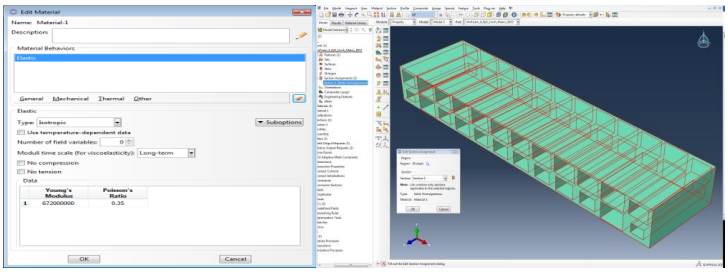

(a) (b)

Figure 6-3 a) Material Properties b) Section Assignment

4. Next step is to mesh the model. Coarse Mesh is preferred since there are lot of void spaces in the structure.

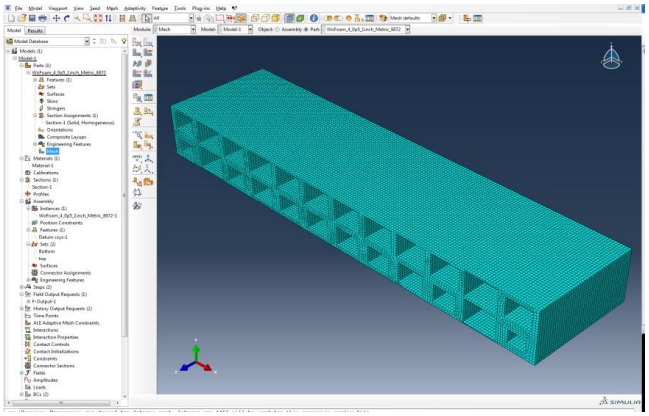

Figure 6-4 Structure after meshing

5. Boundary Conditions are applied.

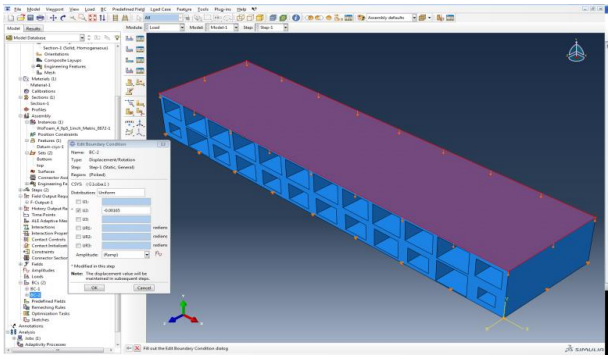

Figure 6-5 Boundary Conditions

6. In history fields, select reaction Force or moments or stress whichever output requires from the analysis

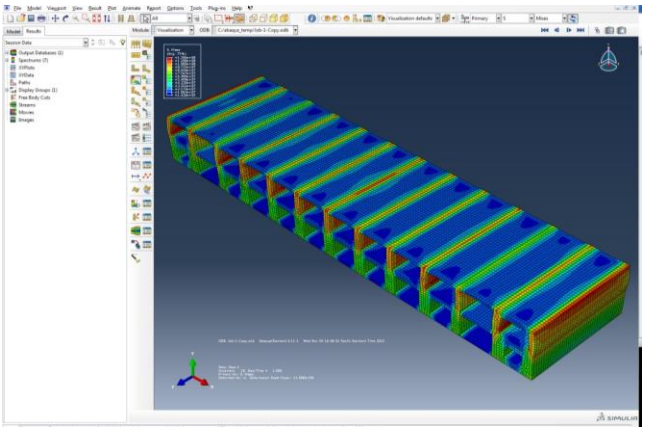

Figure 6-6 Output for Von Mises Stress

7. Same steps were carried out for each simulation.

6-2 Mesh Convergence

In actual theory for each successive level of mesh refinement in the convergence study, all elements in the model should be split in all directions. It is not important that this needs to be carried out on the entire model. St Venant's Principle states that local stresses in one region of a structure do not affect the stresses elsewhere. Therefore, meshing has to be done only in the regions of interest. This is known as local mesh refinement. If a model is required to produce accurate stresses only at certain regions of interest, the role of all elements away from these regions is for only representing geometry and transmitting load [9]. Hence for our analysis mesh was made dense only at the regions of interest.

Figure 6-7 shows the initial mesh and resulting stress acting at the center. In the next analysis the mesh was made denser at the center and stress was calculated as shown in Figure 6-8. This was carried on till the mesh converged. Mesh was converged when even after increasing the number of nodes, the value of stress remains unchanged.

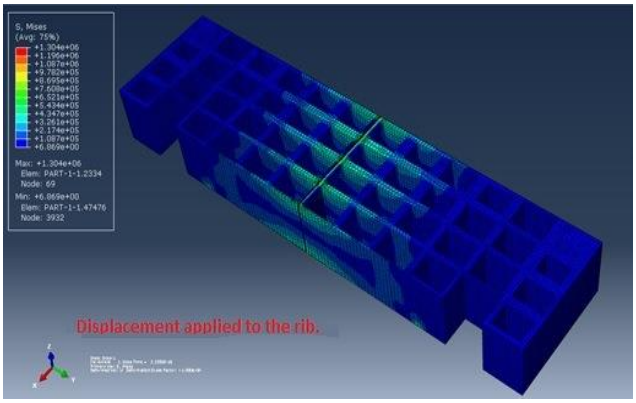

Figure 6-7 Initial mesh and corresponding stress

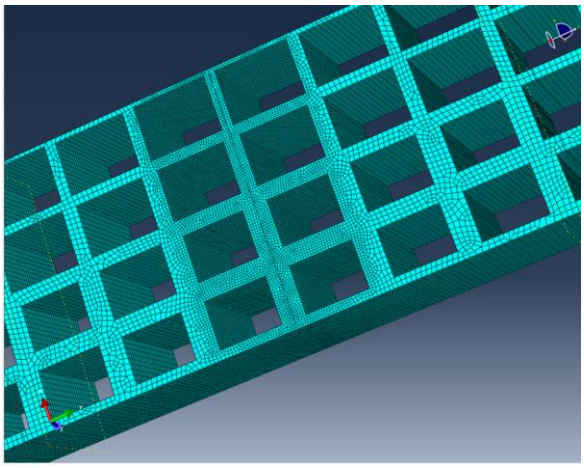

Figure 6-8 Dense Mesh

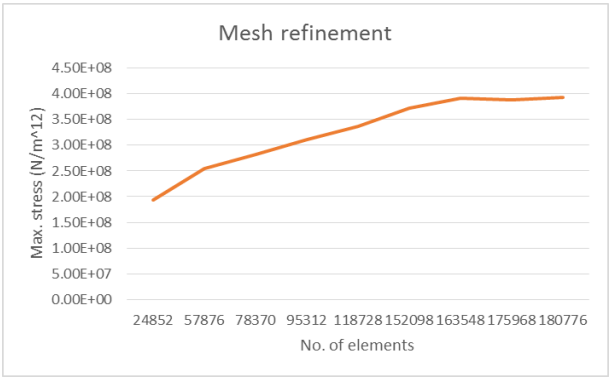

Figure 6-9 Mesh Convergence

6.3 Bending Results and Discussions

For bending analysis, same procedure was followed as defined in section 6.1. Boundary conditions were applied as shown in

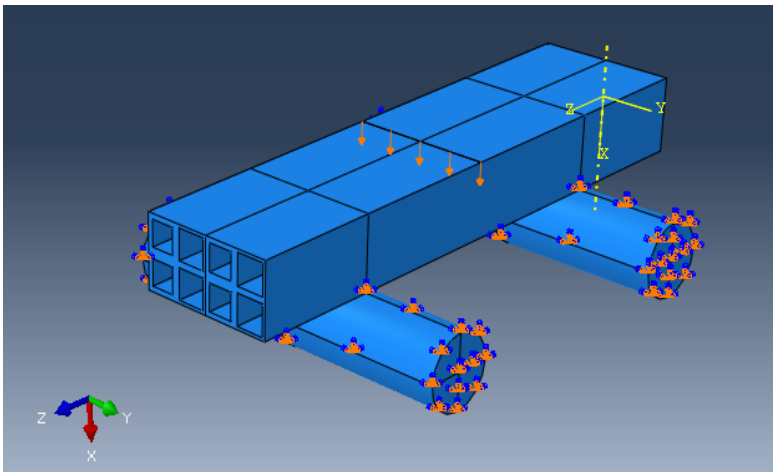

Figure 6-10 Boundary conditions for bending

Mesh convergence was done on the central region where maximum stress was acting as explained in section 6.2. All the forces which were acting on the single line (the line which is displaced by the experimental amount) in the vertical direction were added up. Table 6-1 shows the comparison between ABAQUS and Experimental Results.

Table 6-1 Comparison between ABAQUS and Experimental results

		Force (N)	
		ABAQUS	Experimental
X	Without Foam	480.2	563.73
	With Foam	523.9	569.8427
Y	Without Foam	206.4	202.3172
	With Foam	236.66	331.783
Z	Without Foam	548.1	669.1154
	With Foam	920.1	1408.897

Table 6-1 shows that the results are almost similar and structure in Z-direction can withstand maximum bending force

6.4 Compression Results and Discussion

Compression analysis was done similar to section 6.1. All the forces which were acting on the top face (face which was displaced) was added up. Table 6-2 shows the comparison between ABAQUS and experimental results for compressive force.

Table 6-2 Comparison between ABAQUS and experimental results for compressive force

		Force (N)	
		ABAQUS	Experimental
X	Without Foam	13120	1169.465
	With Foam	13254	1155.149
Y	Without Foam	11850	1045.678
	With Foam	15686	1475.745
Z	Without Foam	40659	1291.371
	With Foam	48598	5000

FEA values are really high as compared to experimental ones. One of the possible reasons for this was the buckling effect which might have taken place during compression. Actual experimental model was built layer by layer as opposed to the solid model which was used for FEA. Hence buckling analysis was performed on all the 3 structures to find out the maximum stress which causes buckling. Maximum compressive strength of ABS is 65 MPa [24]. Buckling equation for fixed- fixed support is defined in Mechanics Theory [25]. Buckling analysis was done on the least thick layer for all the three structures

$$P_{cr} = \frac{4 * \pi^2 * E * I}{L^2}$$

$$\sigma_{cr} = \frac{P_{cr}}{A}$$

Where, E = Young's modulus of material = 672 MPa

I = Moment of inertia of the cross section

A = Area of cross section

L = Height of column

6.4.1 Buckling for void space in X-direction

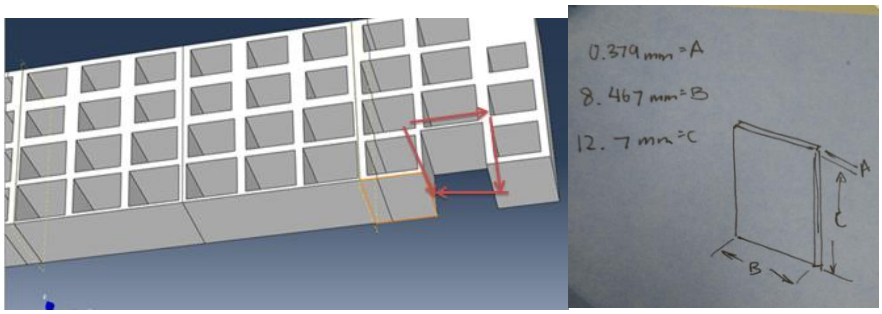

(a) (b)

Figure 6-11 a) Least thickest layer in X-direction b) cross section view of least thickness layer

$$I = \frac{b * a^3}{12}$$

$$= 0.03841 \text{ mm}^4$$

$$E = 672 \frac{N}{mm^2}$$

$$P = \frac{4 * E * I * pi^2}{L^2}$$

$$= 6.25 \text{ N}$$

$$\sigma = \frac{P}{b * a} = 1.95 \text{ MPa}$$

Compressive stress for ABS is 65MPa and hence this structure will undergo buckling.

6.4.2 Buckling analysis for void space in Y-direction

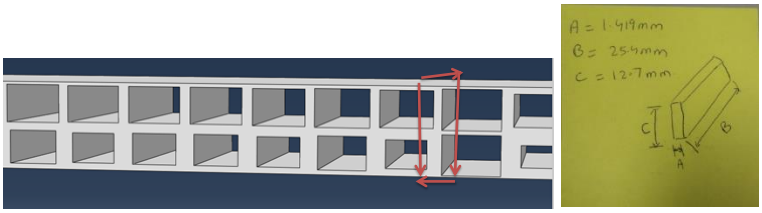

(a) (b)

Figure 6-12 a) Least thickness layer in Y-direction b) cross section view of least thickness layer

$$I = \frac{b * a^3}{12} = 5.8\ mm^4$$

$$E = 672 \frac{N}{mm^2}$$

$$P = \frac{4 * E * I * pi^2}{L^2}$$

$$= 955.34\ N$$

$$\sigma = \frac{P}{b * a} = 26.5\ MPa$$

Compressive Stress for ABS is 65MPa and hence this structure will undergo buckling

6.4.3 Buckling analysis for void space in Z-direction

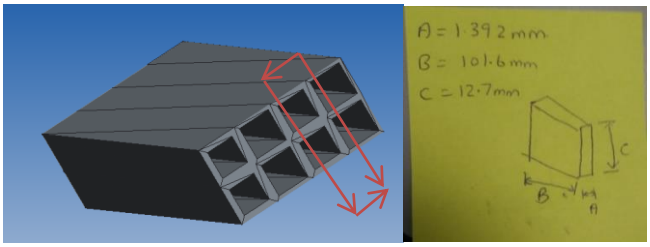

(a) (b)

Figure 6-13 a) Least thickness layer in Y-direction b) cross section view of least thickness layer

$$I = \frac{b * a^3}{12} = 22.7\ mm^4$$

$$E = 672 \frac{N}{mm^2}$$

$$P = \frac{4 * E * I * pi^2}{L^2}$$

$$= 3733N$$

$$\sigma = \frac{P}{b * a} = 26.4MPa$$

Compressive Stress for ABS is 65MPa and hence this structure will undergo buckling

Chapter 7

Conclusion

- The condition for manufacturing was optimized in a MakerBot replicator 2X 3D printer. Optimized condition was number of shells as 2, infill percentage as 100 and layer thickness as 0.15mm. This condition was maintained to manufacture structure throughout this study.
- CT scan image of a 61 year old human femoral joint was used to obtain naturally optimized structure and in house topology optimization tool was used for topology optimized structure. These structures were then converted into a .STL format and using MakerBot software it was converted into .x3g format which was used for printing.
- Polyurethane foam is a light weight and low density material which was used to fill the void spaces in the structures.
- Compression analysis of bone structure shows that its specific strength is highest in the Z-direction filled with polyurethane foam.
- Compression and 3-point bending analysis of topology optimized structures shows that it can bear the maximum bending and compressive force along the Z-direction filled with polyurethane foam. Hence structure in Z- direction should be used in all applications were light weight and high load bearing capacity structures are needed
- When a compressive force is applied to a cellular structure, it breaks before it reaches its compressive strength due to buckling. Polyurethane foam helps to avoid buckling and gives us a true compressive strength of the structure.
- Finite Element analysis gives almost same result as the experimental ones for bending. During compression, the actual structure was built layer by layer as

opposed to a complete solid model which was used for analysis. Actual structure undergoes buckling and hence the experimental and FEA results differs.

7.1 Future Work

- In the present study bone like structures were manufactured with ABS plastic. In the future study, it should be manufactured with a biodegradable material.
- Polyurethane foam is not a biodegradable material and hence it should be replaced with a biodegradable material for medical applications.
- MakerBot replicator 2X was a very basic form of 3D printer. For future study these structures should be manufactured with a better 3D printer which has a high resolution.

References

1. Witkiewicz, W. (2006). PROPERTIES OF THE POLYURETHANE LIGTH FOAMS .

2. Olczyk W.: Poliuretany. WNT, Warszawa, 1968.

3. www.ruuki.com.pl

4. www.balex.com.pl

5. www.generalplastics.com/products/idatasheets.php

6. Jane Lian, J. G. (2014). Bone Structure and Function .

7. Muler, R. (n.d.). Bone Structure and Function. Switzerland.

8. Md.Sarkar Farzad, ”Degradation Mechanics of Bone and Bone like Materials via Multiscale Analysis”Dissertation, Doctor of Philosophy, University of Texas, Arlington.

9. The Importance of Mesh Convergance- 1. (n.d.). Retrieved from NAFEMS: http://www.nafems.org/join/resources/knowledgebase/001/

10. Sajth Anantharaman, “TOPOLOGY OPTIMIZATION FOR THIN WALLED STRUCTURES UTILIZING SIMP METHOD BY ADDITIVE MANUFACTURING USING OPTIMIZED CONDITIONS”, Master of Science, University of Texas, Arlington

11. Gibson, L. J.; Ashby, M. F. (1997) Cellular Solids: Structure and Properties, Cambridge University Press, Cambridge, UK.

12. Jane. Chu, S. E. A Comparison of Synthesis Methods for Cellular Structures with Application to Additive Manufacturing.

13. Sushma Pothana, “Manufacturing and Characterization of Ultra Light Bio-Inspired Nanocomposite Structures”, Master of Science, University of Texas, Arlington

14. Yang, L. Experimental assisted design development for a 3D reticulate octahedral cellular structure using additive manufactuing .

15. Lorna J. Gibson. Cellular solids: structure and properties, 2nd edition. Cambridge University Press, New York, NJ, USA. 1997

16. M.F. Ashby, A. G. Evans, N. A. Fleck, L. J. Gibson, J. W. Hutchinson, H. N. G. Wadley. Metal Foams: A Design Guide. Butterworth-Heinemann, Boston, US. 2000.

17. O. Cansizoglu, O, Harrysson, D. Cormier, H.West, T. Mahale. Properties of Ti-6Al-4V non-stochastic lattice structures fabricated via electron beam melting. Materials Science and Engineering: A, 492(2008), 1-2: 468-474.

18. L. Yang, D. Cormier, H. West, K. Knowlson. Non-stochastic Ti6Al4V foam structure that shows negative Poisson's Ratios. Materials Science and Engineering: A, 558(2012): 579-585.

19. Jens Bauer, Stefan Hengsbach, Iwiza Tesari, Ruth Schwaiger, Oliver Kraft. High-strength cellular ceramic composites with 3D microarchitecture. Proceedings of the National Academy of Sciences of the United States of America. 111(2014), 7: 2453-2458.

20. 3D printed nanostructured materials. http://www.engineering.com/3DPrinting/3DPrintinArticles/ArticleID/7832/3D-Printed-Nanostructured-Materials-Are-Strong-Light-Have-Many-Uses.aspx.

21. Li Yang. Lightweight cellular structures with additive manufacturing: New design freedoms. RAPID Conference and Exposition. Detroit, USA, 2014.

22. Part 1 – Francis MacLachlan: Student and Shipyard Days. (2015). Retrieved from Curiouslakecurator's Blog: http://curiouslakescurator.net/2015/06/06/part-1-francis-maclachlan-student-and-shipyard-days/

23 History of 3D printing: the Free begineer's Guide. (2014, MAY). Retrieved from 3D Printing Industry: 3dprintingindustry.com/3d-printing-basics-free-beginners-guide/history/

24. Compressive Strength Testing of Plastics. (n.d.). Retrieved from MatWeb: http://www.matweb.com/reference/compressivestrength.aspx

25. Gramoll, K. Column Buckling. In Mechanical Theory.

Biographical Information

Sachin Jose was born and bought up in Mumbai, India. He received Bachelor's degree in Mechanical Engineering from University of Mumbai in May 2013. He moved to Arlington, Texas in January 2014 to pursue his Master of Science degree. He started working with Dr Adnan Ashfaq from June 2014. His research focuses on stress analysis of naturally and artificially obtained cellular structures. He has previous work experience as supervisor at Domech Fabricators and as a mechanical engineer co-op at St Jude Medical.